

Deep crustal structure of the North Anatolian Fault and the earthquake cycle

Dense Array for Northern Anatolia

Sebastian Rost¹, Gregory Houseman¹, David Thompson^{1,2}, David Cornwell²

¹School of Earth and Environment, University of Leeds, Woodhouse Lane, Leeds, LS2 9JT

²School of Geosciences, University of Aberdeen, King's College, Aberdeen, AB24 3UE

1. Abstract

A passive seismic experiment was conducted across the North Anatolian Fault Zone in the region of the rupture of the 1999 Izmit earthquake ($M=7.6$). The project aimed to resolve the fine scale crustal structure of the Fault Zone using scattered seismic waves. The 63 autonomous seismic stations were deployed on a regular grid covering approximately 35 by 70 km with a nominal station spacing of 7 km. The network also included 3 permanent stations of the Turkish National Earthquake Monitoring Network. The network was augmented by 7 autonomous seismic stations forming a semi-circle around the dense array and provided by the Kandilli Observatory and Earthquake Research Institute (KOERI). Stations were recording continuously at 50Hz sampling rate between May 2012 and September 2013. The data quality of DANA was generally good despite many stations being deployed in industrial and heavily populated areas. Data recovery across the whole network (including KOERI stations, but not permanent stations) was excellent with an average data recovery of 94%. The data from DANA offers opportunity for a multitude of analysis methods. Analysis of the data is ongoing, but several initial results are in revision or have been published. These include a detailed receiver function analysis, local earthquake detection and location and resolution of crustal structure from transfer functions.

2. Background

The North Anatolian Fault Zone (NAFZ) is a major continental strike-slip fault system located in northern Anatolia. Relative motion across this fault occurs at an average speed of 20-30 mm/yr and the fault is the main focus of deformation on the northern edge of the Anatolian region as it moves west toward the Hellenic subduction zone. The fault accommodated 12 large earthquakes ($M=6.7$ and above) since 1939 and the dominantly westward movement of strong seismicity along the fault poses a large hazard of a future strong earthquake in the Istanbul region.

The main aim of this multidisciplinary NERC funded project is to develop a crustal scale model of the NAFZ that is consistent with the cumulative strain history indicated by seismic images of fault zone structure and geological measurements of petrophysical properties, and the short-term strain history constrained by geodetic data. The particular objective of the seismic component of the project was to image the fine-scale crustal structure of the North Anatolian Fault Zone.

3. Survey Procedure

Approximately 18 months of continuous data were collected at 63 locations deployed on a semi-regular grid covering an area of approximately 35 km by 70 km (Figure 1). Station equipment included 61 x CMG-6TDs, 6 x CMG-3TD, 2 x CMG-3ESPD and 1x CMG-40T. The CMG-3TD sensors were deployed at the corners of the DANA grid and close to the northern strand of the NAFZ (DA01, DA07, DA11, DF01, DF06, DF11). A single CMG-40T sensor was deployed at location DD02 and the CMG-3ESP sensors were deployed at DA08 and DF07. All other station locations were equipped with CMG-6TD sensors. A substantial fieldwork programme was necessary to install and maintain these stations. The fieldwork programme would not have been possible without the support of the project partners at KOERI and Sakarya University.

Site Allocation and Permission (Jan/Mar 2012)

Staff from the University of Leeds (Houseman, Rost, Thompson) and KOERI (Turkelli, Teoman, Kahraman) visited the field area twice to get permission for station deployment from local landowners close to the theoretical gridpoints. Where possible, stations were deployed on private land for improved station security. For each site advice was sought from the local Mukhtar (local village official). Landowners were met in person and the best location was determined. Most locations were dependent on solar power and clear view of the southern sky was essential and achieved in most cases. Only a minority of stations relied on mains power mainly in KOERI vaults. All of the landowners were eager to give permission for seismometers to reside on their land and in general very cooperative.

Deployment (May 2012)

Staff from the University of Leeds, Seis-UK (Lane), KOERI, and Sakarya University were involved in the deployment phase. Pre-deployment testing and deployment operated out of Sakarya University, which also provided housing for deployment staff. Most of the seismic instruments were shipped from Seis-UK using DespatchPoint and delivered to Sakarya University. Sixteen sensors were shipped directly from Güralp Systems Ltd after delays in the memory upgrade for these instruments. Sundry materials including batteries, tools, and station building supplies were purchased locally. All instruments were tested and made ready for deployment at Sakarya University. Four deployment teams installed 67 of the stations within 10 days with the remaining 3 stations (KO) being deployed by KOERI staff shortly afterwards. Seis-UK deployment advice was followed. At most locations deployment on bedrock was not possible. Stations with CMG-6TD sensors were deployed on slabs placed about 1 m deep in back-filled ground holes. Where on bedrock, quick setting cement was used to fixate the plate. The sensor was protected in a plastic bag, an inverted plastic basin was placed above the sensor before burial to protect sensor and cables and the sensor hole was covered with plastic covered plywood. Framed solar panels were deployed on a single pole also holding the GPS antenna (Fig. 2). Battery and break-out box were protected in partly buried, ply-wood covered storage boxes. GPS and power cables were protected using flexible irrigation tubing. Stations with CMG-3T, CMG-3EPSD and CMG-40T were installed in a large diameter irrigation tube on a sand levelled slab, again in most situations above bedrock. The tubes were not backfilled. Solar panels were installed using an A-frame installation. If deemed necessary stations were secured through simple fencing. At each station a sign informed about the sensitivity of the seismic equipment and gave contact information of the KOERI collaborators. Ground motion was recorded with a sampling rate of 50Hz and a 1Hz status stream was also recorded to aid fast station health checks.

Service Trips and Decommissioning

All stations were visited regularly during service trips in September 2012, November 2012, March 2013, and September 2013. Data were recovered to portable hard disks following Seis-UK procedures. Any power and GPS issues were resolved during these visits. In rare cases CMG-6D instruments were exchanged with a spare instrument. In agreement with Seis-UK, defect CMG-6D instruments were serviced at Güralp's Izmit service location avoiding shipping instruments back to the UK. Service in Turkey was quick, reliable and convenient. One station with ongoing and unresolvable short-term issues for most of the deployment was DF11 (CMG-3T) and these were identified as GPS and power issues. Stations DB07, DD09 DD10, DD11, DF06, DF08, DF09 showed power issues with short term (night) data loss mainly during the winter months, with DB07 and DF11 also showing summer power outages due to foliage cover of the solar panel. There were no significant problems with station security or equipment stolen, with one case of possible vandalism where a solar panel cable was detached from the panel.

4. Data Recovery and Quality

Data recovery was calculated at approximately 94% for the stations of the DANA array (Figure 1). Data were lost due to power issues, mainly due to insufficient solar exposure and snow cover in winter and a few instrument issues as discussed above. Data quality varies across the array with higher noise levels especially in the north-east and the sediment basins along the Sakarya River, and in the Izmit area. Data quality was in general better than expected. For such a large network relatively few instrument issues were encountered and the data recovery was deemed excellent.

5. Interpretation to Date

A multitude of different analysis techniques have already been implemented on the DANA data set. Several publications (Altuncu Poyraz et al., 2015; Frederiksen et al., 2015; Kahraman et al., 2015) have been published or are in revision. Several other analysis projects are ongoing and publications are in preparation. Results will be presented in peer-reviewed publications and have been presented in numerous conference presentations.

Receiver Functions

Receiver function (RF) analysis is a common technique to study the crustal structure beneath distributed stations using teleseismic earthquake energy. DANA allows a very dense sampling of the seismic wavefield and allows very high resolution of the crustal structure in the region of the DANA stations (Figure 3). Traditional H- κ stacking and common conversion point (CCP) migration are applied (Kahraman et al., 2015). The analysis finds striking lateral changes in crustal structure on scale lengths of less than 10 km both in North-South direction over the northern and southern branch of the NAFZ as well as in East-West direction in the different crustal terranes (Figure 4).

Crustal transfer functions

Crustal transfer functions (Frederiksen et al., 2015) remove the need for deconvolution for source normalization avoiding common problems with crustal-scale RF analysis and allow better resolution of especially shallow crustal structure such as sediment basins. The analysis of the DANA data shows evidence for two thick zones of sedimentary material north of the northern fault zone and straddling the southern branch. Crustal thickness increases sharply north of the northern strand of the NAFZ, while the P-wave to S-wave velocity ratio changes across the southern strand indicating that the NAFZ follows pre-existing geological boundaries rather than being aligned with the stress field. The study also indicates a mantle contribution to the isostatic equilibrium north of the northern NAFZ.

Local seismicity

The dense seismic network allowed the detection of 2437 seismic events from May 2012 to September 2013 (Figure 5). The analysis shows that 1371 of these are earthquakes with the remainder related to quarry explosions (Altuncu Poyraz et al., 2015). The magnitude threshold for these events is $M_L = 0.1$ with horizontal and vertical uncertainties not exceeding 0.8 and 0.9 km, respectively. Focal mechanism solutions confirm that Sakarya and its vicinity is stressed by a compressional regime showing a primarily oblique-slip motion character. Stress tensor analysis indicates that the maximum principal stress is aligned in WNW-ESE direction and the tensional axis is aligned in NNE-SSW direction.

Other analysis

Several other projects analyse this outstanding dataset. These include scattering migration (Aberdeen, Bergen, Leeds), scattering tomography (Leeds, Aberdeen, Winnipeg), S-wave receiver functions (Aberdeen, Leeds), local tomography (KOERI, Leeds), deep Earth structure (Leeds), local and teleseismic anisotropy (Leeds, Aberdeen) and anisotropic receiver functions (Aberdeen, Leeds). The dataset has been used in several senior undergraduate projects and for summer internships for UK and EU students and is also analysed within 2 PhD projects located in Aberdeen (P_n tomography – University of Aberdeen funded) and Leeds (ambient noise tomography – NERC DTP funded).

6. Conclusions and Recommendations

In conclusion the seismic field experiment was highly successful and produced a unique dense sampling of the seismic wavefield. The scientific objectives of the funded research will be achieved. Nonetheless we would like to comment on the following points:

- The project incurred excessive shipping and customs charges due to the late shipping of refurbished instruments and difficulties with the shipping agent in Turkey. Clearer shipping charges and better advice on customs regulations would have been helpful.
- DANA included a mix of instruments with the CMG-6TD being relatively noisy. Although the simplicity of the CMG-6TD deployment allowed for quick installation a larger pool of quiet instruments (CMG-3 variants, STS-2) would help the science especially for these very dense installations.
- Although flooding problems were rare (3 sensors) with backfilled sensor holes, a test of noise conditions for several deployment methods could inform PIs further which installation method to use.
- The purchasing of sundries in Turkey required a full seven days by several team members to source all the requirements but was an easy and cost-effective way to source station building equipment.
- Acquiring data at 50 Hz and 1 Hz sampling rate was very useful to QC data in the field. The 50 Hz sampling rate could have been adjusted to 100 Hz due to the instrument memory upgrade.
- The installation of this network would have been impossible without the support of our local partners at the Kandilli Observatory and Earthquake Research Institute and Sakarya University.

7. Data Archive

All data have been archived at Seis-UK and have been uploaded to the IRIS DMC running through all IRIS data and metadata tests. Data are currently embargoed.

8. References

- Altuncu Poyraz, S., Teoman, M.U., Turkelli, N., Kahraman, M., Cambaz, D., Mutlu, A., Rost, S., Houseman, G.A., Thompson, D.A., Cornwell, D.G., Utkucu, M., Gulen, L., 2015. New constraints on micro-seismicity and stress state in the western part of the North Anatolian Fault Zone: Observations from a dense seismic array. *Tectonophysics in revision*.
- Emre, O., Duman, T.Y., Ozalp, S., Elmaci, H., Olgun, S., Saroglu, F., 2013. Active fault map of Turkey with an explanatory text 1:1,25,000.
- Frederiksen, A.W., Thompson, D.A., Rost, S., Cornwell, D.G., Gulen, L., Houseman, G.A., Kahraman, M., Poyraz, S.A., Teoman, U.M., Turkelli, N., Utkucu, M., 2015. Crustal thickness variations and isostatic disequilibrium across the North Anatolian Fault, western Turkey. *Geophys. Res. Lett.* 42, 2014GL062401. doi:10.1002/2014GL062401
- Kahraman, M., Cornwell, D.G., Thompson, D.A., Rost, S., Houseman, G.A., Turkelli, N., Teoman, M.U., Altuncu Poyraz, S., Utkucu, M., Gulen, L., 2015. Crustal-scale shear zones and heterogeneous rheology beneath the North Anatolian Fault Zone, Turkey, revealed by a high-density seismometer array. *Earth Planet. Sci. Lett.* in revision.

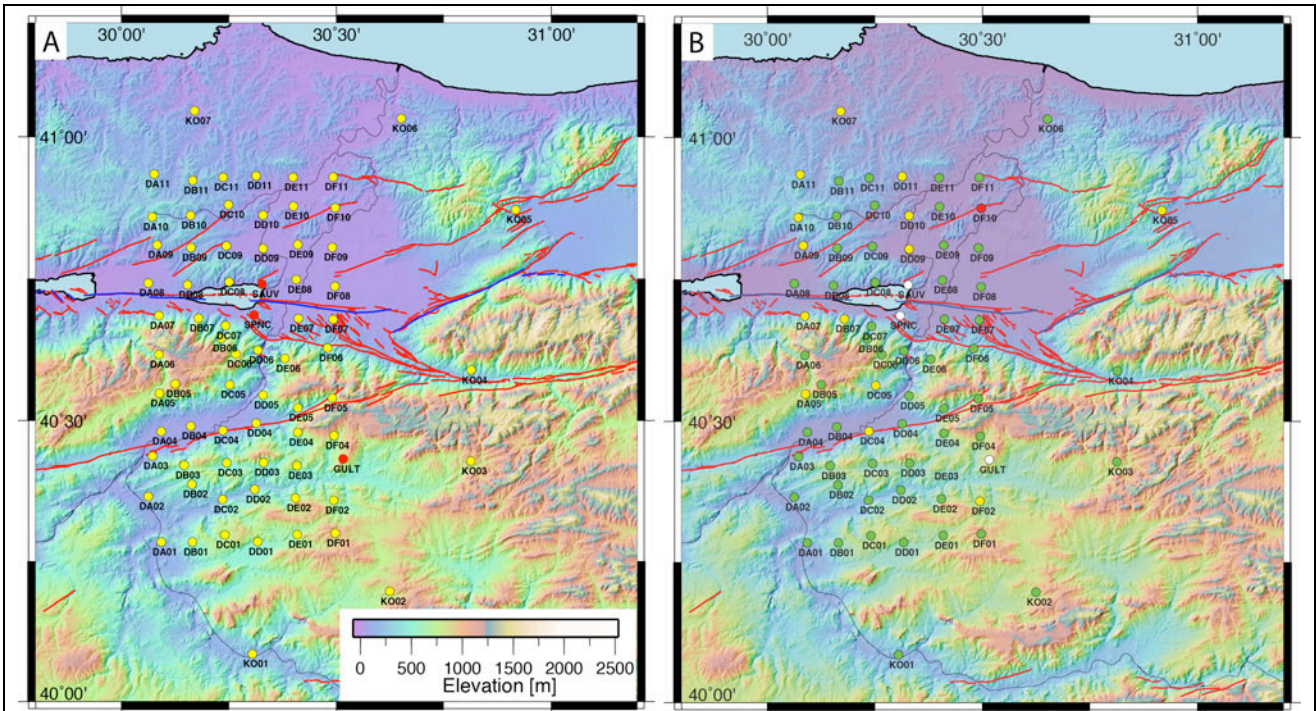


Figure 1 – **A** Deployed station locations (yellow circles) of the DANA array. Background shows the digital elevation model of the SRTM. Three permanent stations (red circles) of the KOERI national network have been included into the network. Stations equipped with Seis-UK equipment in the regular grid of the array have been augmented by 7 stations provided by KOERI (KO01 to KO07) forming a semi-circle around the dense seismic grid. Nominal station spacing is 7 km and has been achieved in most areas of the network. **B** DANA data recovery. Data recovery > 90% (Green), 60% - 90% (amber), < 60% (red). Data recovery of permanent stations (white) is not shown.



Figure 2 - Typical station installation with security fence at station DA09 (CMG-6TD installation). GPS and solar power cables were secured in the yellow flexible piping. The sensor is located in a plastic bag and deployed in a back-filled hole with an inverted small washbasin for increase safety. The sensor hole is covered by plastic covered ply-wood. Battery, cables and break out box are protected in a lid and ply-wood covered storage box.

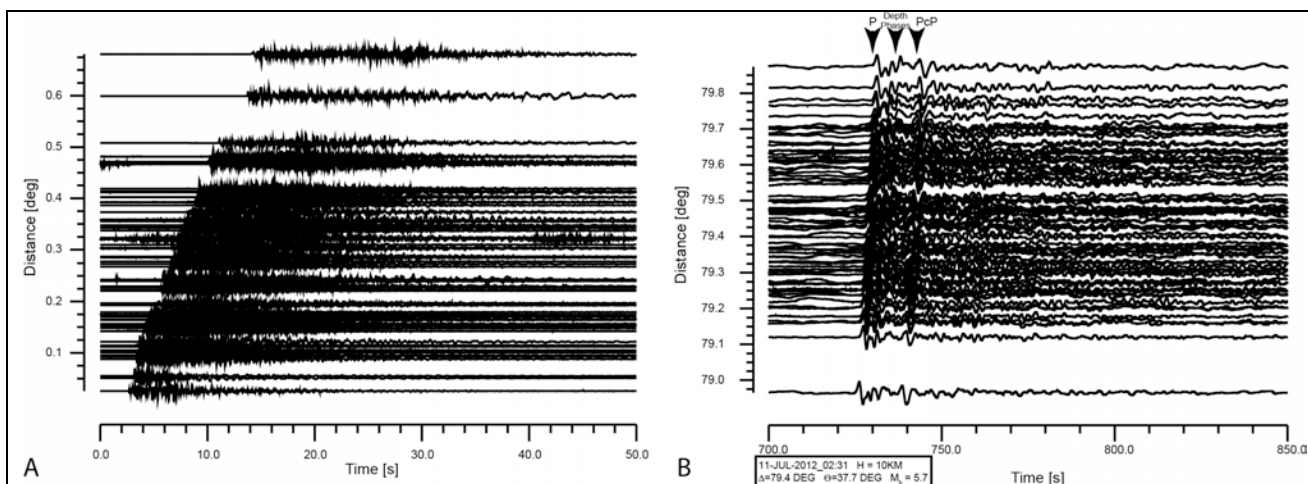


Figure 3 – **A** Data example of a $m_L=4.1$ local event occurring on 07-JUL-2012_07:07:45 close to station DE08 (Serdivan) (Altuncu Poyraz et al., 2015). Traces are aligned on the origin time and traces are sorted by epicentral distance. **B** Data example of a $m_L=5.7$ teleseismic event occurring on 11-JUL-2012_02:31 in the Kuriles. Traces are aligned on the origin time and traces are sorted by epicentral distance. Broad band data were filtered with a low pass Butterworth filter of order 3 with a corner frequency of 1 Hz. Data show excellent coherency of major arrivals across the array with minor coherent phases in the P coda. Signal-to-Noise ratio of most of the stations is excellent.

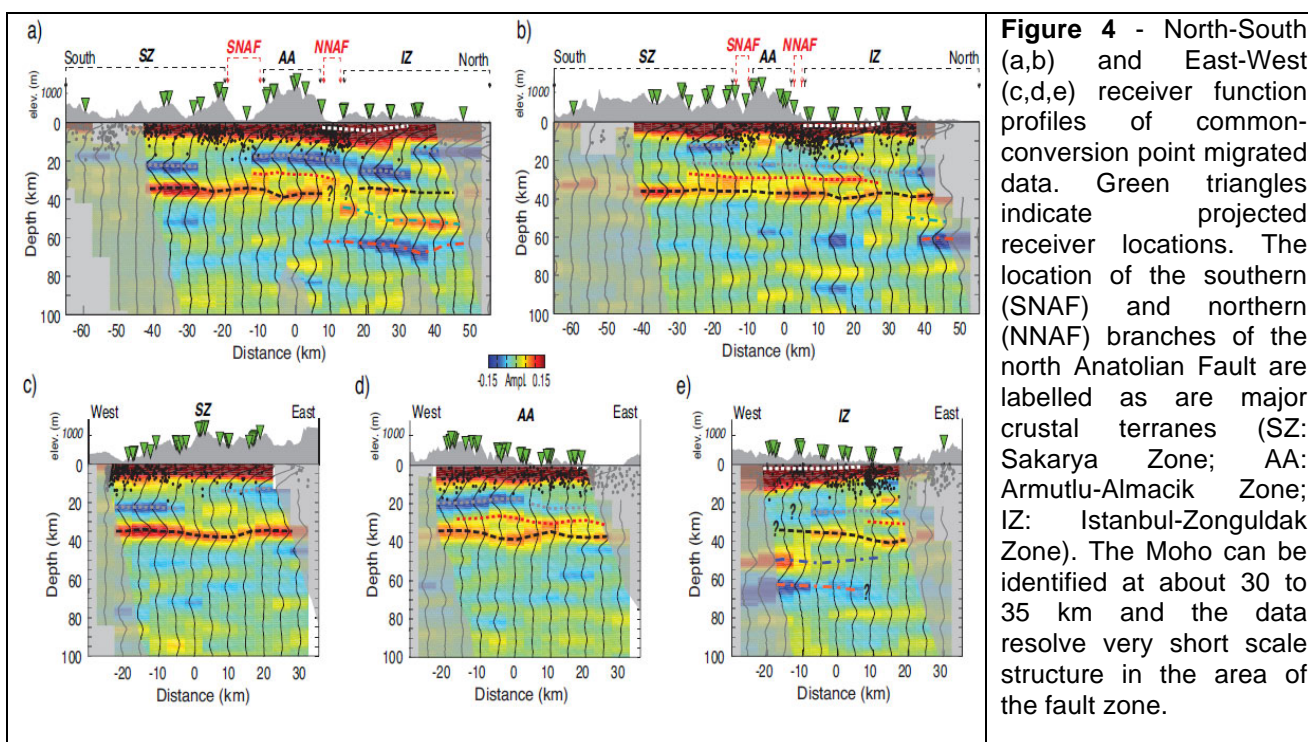


Figure 4 - North-South (a,b) and East-West (c,d,e) receiver function profiles of common-conversion point migrated data. Green triangles indicate projected receiver locations. The location of the southern (SNAF) and northern (NNAF) branches of the north Anatolian Fault are labelled as are major crustal terranes (SZ: Sakarya Zone; AA: Armutlu-Almacik Zone; IZ: Istanbul-Zonguldak Zone). The Moho can be identified at about 30 to 35 km and the data resolve very short scale structure in the area of the fault zone.

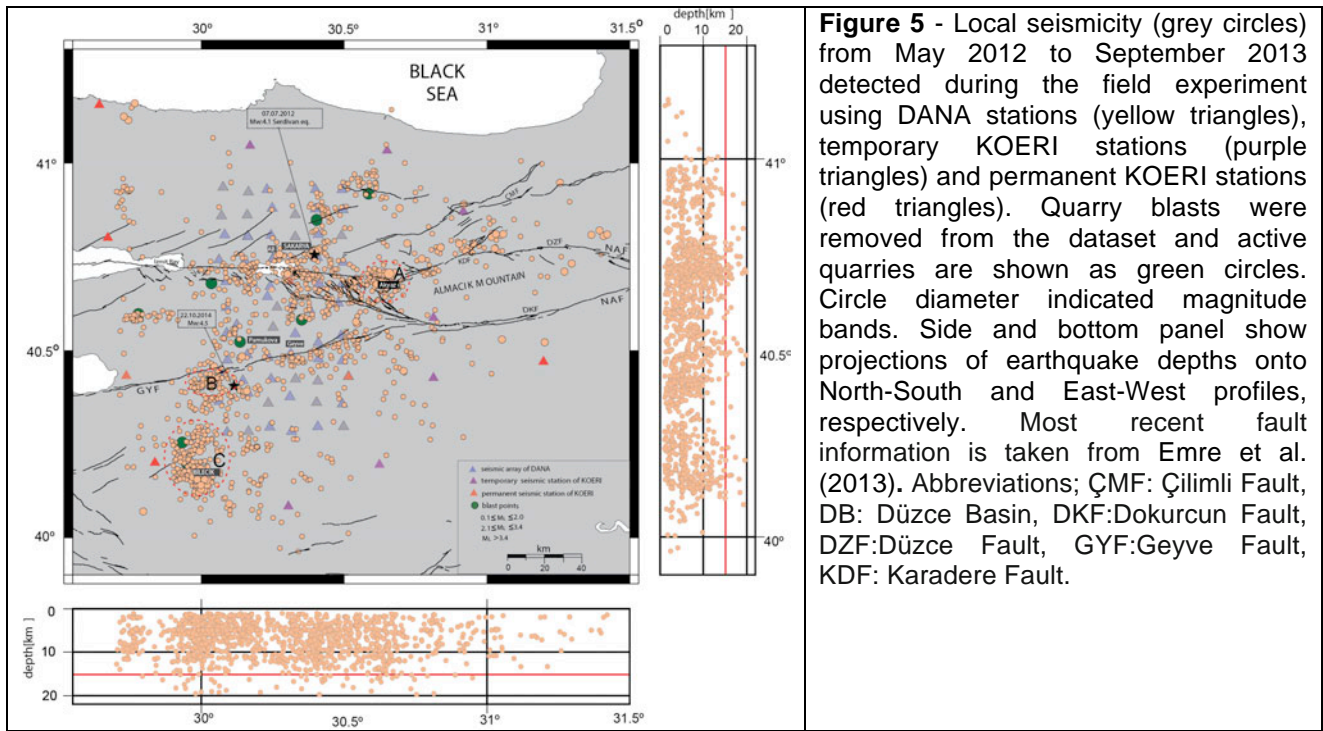


Table 1: Station locations and elevations of all deployed stations as well as the affiliated KOERI stations (KO) and the incorporated permanent station (SAUV, SPNC, GULT).

Station Code	Latitude [deg]	Longitude [deg]	Elevation [m]	Station Code	Latitude [deg]	Longitude [deg]	Elevation [m]
DA01	40.2844	30.09233	195	DD01	40.28501	30.3167	573
DA02	40.36518	30.06197	189	DD02	40.37774	30.31018	269
DA03	40.43722	30.07194	202	DD03	40.42557	30.33016	603
DA04	40.48057	30.09218	77	DD04	40.49533	30.31339	140
DA05	40.54816	30.08835	1004	DD05	40.54522	30.32943	400
DA06	40.61562	30.08697	780	DD06	40.62354	30.31777	182
DA07	40.68465	30.08682	251	DD09	40.80326	30.32908	21
DA08	40.74207	30.06188	50	DD10	40.8621	30.32933	29
DA09	40.80948	30.08269	134	DD11	40.93145	30.31317	114
DA10	40.85926	30.07119	422	DE01	40.29745	30.40881	629
DA11	40.93477	30.07615	259	DE02	40.36204	30.40437	788
DB01	40.28446	30.1652	606	DE03	40.42003	30.40837	683
DB02	40.38702	30.16343	522	DE04	40.47908	30.41037	798
DB03	40.42117	30.14596	526	DE05	40.52236	30.4098	532
DB04	40.49003	30.1612	72	DE06	40.60913	30.37994	470
DB05	40.56492	30.12463	1153	DE07	40.67966	30.41154	40
DB06	40.64467	30.23201	311	DE08	40.74856	30.40647	31
DB07	40.68021	30.17881	425	DE09	40.80975	30.4098	27
DB08	40.73931	30.15336	121	DE10	40.87793	30.40003	15
DB09	40.80496	30.16194	210	DE11	40.92894	30.39881	69
DB10	40.86179	30.16051	247	DF01	40.30035	30.49719	969
DB11	40.9229	30.16578	200	DF02	40.35849	30.49383	744
DC01	40.29688	30.24054	717	DF04	40.4734	30.49432	924
DC02	40.35988	30.23488	195	DF05	40.5399	30.49023	728
DC03	40.42487	30.24454	455	DF06	40.62751	30.47924	200
DC04	40.48245	30.23563	90	DF07	40.6782	30.49256	129
DC05	40.56345	30.25181	249	DF08	40.73641	30.4963	26
DC06	40.61672	30.26575	555	DF09	40.80557	30.49024	24
DC07	40.66708	30.24217	164	DF10	40.87526	30.49721	30
DC08	40.74444	30.25013	162	DF11	40.92927	30.49252	45
DC09	40.80777	30.24419	82	KO01	40.08489	30.30434	216
DC10	40.88017	30.24904	152	KO02	40.19659	30.62442	881
DC11	40.92865	30.23644	167	KO03	40.42811	30.81314	915
DD01	40.28501	30.3167	573	KO04	40.58879	30.81337	577
DD02	40.37774	30.31018	269	KO05	40.87158	30.91747	187
DD03	40.42557	30.33016	603	KO06	41.03235	30.65097	114
DD04	40.49533	30.31339	140	KO07	41.0459	30.1702	68
DD05	40.54522	30.32943	400	SAUV	40.7401	30.3271	165
DD06	40.62354	30.31777	182	SPNC	40.686	30.3083	190
DD09	40.80326	30.32908	21	GULT	40.432	30.5156	942

Peer-reviewed Publications

- Altuncu Poyraz, S., Teoman, M.U., Turkelli, N., Kahraman, M., Cambaz, D., Mutlu, A., Rost, S., Houseman, G.A., Thompson, D.A., Cornwell, D.G., Utkucu, M., Gulen, L., 2015. New constraints on microseismicity and stress state in the western part of the North Anatolian Fault Zone: Observations from a dense seismic array. *Tectonophysics in revision*.
- Frederiksen, A.W., Thompson, D.A., Rost, S., Cornwell, D.G., Gulen, L., Houseman, G.A., Kahraman, M., Poyraz, S.A., Teoman, U.M., Turkelli, N., Utkucu, M., 2015. Crustal thickness variations and isostatic disequilibrium across the North Anatolian Fault, western Turkey. *Geophys. Res. Lett.* 42, 2014GL062401. doi:10.1002/2014GL062401
- Kahraman, M., Cornwell, D.G., Thompson, D.A., Rost, S., Houseman, G.A., Turkelli, N., Teoman, M.U., Altuncu Poyraz, S., Utkucu, M., Gulen, L., 2015. Crustal-scale shear zones and heterogeneous rheology beneath the North Anatolian Fault Zone, Turkey, revealed by a high-density seismometer array. *Earth Planet. Sci. Lett.* in revision.

Presentations

- Rost et al. (invited)**, The crustal structure along the 1999 Izmit/Düzce rupture of the North-Anatolian Fault, EGU General Assembly, EGU2015-9998, 2015.
- Wright et al. (invited)**, The Earthquake Loading Cycle and the Deep Structure of the North Anatolian Fault, AGU Fall Meeting, G13B-07, 2014.
- Teoman et al.** New Insights on Seismicity and the Velocity Structure beneath the Western Segment of the North Anatolian Fault Zone, AGU Fall Meeting, S21E-05, 2014
- Frederiksen et al.**, Crustal and Basin Thickness Via P-Coda Transfer Functions: Examples from the Southwestern Superior Province, USA and the North Anatolian Fault, Turkey, AGU Fall Meeting, S22B-02, 2014
- Cornwell et al.**, Abrupt variations in brittle-ductile transition depth and lower crustal properties beneath two branches of the north Anatolian fault zone, Turkey, AGU Fall Meeting, T22A-04, 2014
- Thompson et al.**, High resolution images of the mid- to lower-crust beneath the North Anatolian Fault obtained using the scattered seismic wavefield, AGU Fall Meeting, T13A-4626, 2014
- Teoman et al.**, Crustal Anisotropy Beneath the Western Segment of North Anatolian Fault Zone from Local Shear-Wave Splitting, AGU Fall Meeting, S21C-4461, 2014
- Cornwell et al.**, Detailed Northern Anatolian Fault Zone crustal structure from receiver functions, AGU Fall Meeting, T23E-2633, 2013.
- Thompson et al.**, Imaging the North Anatolian Fault using the scattered teleseismic wavefield, AGU Fall Meeting, T22D-07, 2013.
- Turkelli et al.**, Seismicity and Crustal Anisotropy Beneath the Western Segment of the North Anatolian Fault: Results from a Dense Seismic Array, AGU Fall Meeting, T22D-06, 2013
- Yamasaki et al.**, Weak ductile shear zone beneath the western North Anatolian Fault Zone: inferences from earthquake cycle model constrained by geodetic observations, AGU Fall Meeting, T23E-2634, 2013
- Wright et al.**, The Earthquake Loading Cycle and the Deep Structure of the North Anatolian Fault, EGU General Assembly, EGU2014-11223, 2014.